PFC/JA-86-25

Gyrotron Powered Electromagnetic Wigglers for Free Electron Lasers

B.G. Danly, G. Bekefi, R.C. Davidson
R.J. Temkin, T.M. Tran†, and J.S. Wurtele
Plasma Fusion Center
and
Department of Physics
Massachusetts Institute of Technology
Cambridge, MA 02139

April 1986

Submitted to the IEEE Journal of Quantum Electronics

† Permanent Address: CRPP, Association Euratom-Confederation Suisse, EPFL 21., Av. des Bains, CH-1007, Lausanne, Switzerland

Abstract

The operation of free electron lasers (FELs) with axial electron beams and high power electromagnetic wiggler fields such as those produced by high power gyrotrons is discussed. The use of short wavelength electromagnetic wigglers in waveguides and resonant cavities can significantly reduce required electron beam voltages, resulting in compact FELs. Gain calculations in the low and high gain Compton regime are presented, including the effects of emittance, transverse wiggler gradient, and electron temperature. Optimized scaling laws for the FEL gain and the required electromagnetic wiggler field power are discussed. Several possible configurations for FELs with electromagnetic wigglers powered by millimeter wavelength gyrotrons are presented. Gyrotron powered wigglers appear promising for operation of compact FELs in the infrared regime using moderate energy (< 10 MeV) electron beams.

I. INTRODUCTION

The ubitron/free electron laser (FEL) has been shown to be a promising source of radiation over a broad range of frequencies from the optical to the millimeter range [1-10]. Recent experimental progress has included the generation of high frequencies using rf linear accelerators [1,2,5] and storage rings [3], and the generation of high power in the millimeter band with high efficiencies using linear induction and pulse line accelerators [4,7-10]. Operation of an FEL based on an electrostatic accelerator has produced radiation in the far infrared [6].

For relativistic electron beams, the resonance condition for the conventional FEL with a magnetostatic wiggler can be expressed as $k_s = 2\gamma^2 k_w(1 + a_w^2)^{-1}$, where $k_s(k_w)$ is the optical (wiggler) wave number, γ is the relativistic factor, $\gamma = (1-\beta_\perp^2 - \beta_\parallel^2)^{-1/2}$, and a_w is the normalized vector potential of the wiggler magnetostatic field, B_w ($a_w = eB_w/mc^2k_w$). Because the wavelength of magnetostatic wiggler fields is usually limited to $\lambda_w = 2\pi/k_w \geq$ 2 cm, the conventional FEL requires high energy electron beams typically in excess of 40 MeV to reach the visible and near IR portions of the spectrum.

An alternate concept to the conventional FEL which has received both considerable experimental and theoretical attention recently is the use of an electromagnetic wave as the wiggler rather than the field from a magnetostatic wiggler [11-16]. In this case, if the wiggler wave is propagating in free space, the resonance condition becomes $k_s = 4\gamma^2 k(1+a_w^2)^{-1}$, where k is now the wave number of the electromagnetic wave. The ability to use short wavelength electromagnetic waves as the wiggler field would allow a substantial reduction of the beam energy necessary for obtaining any given laser frequency. FEL operation at lower beam energy has many major technological implications, including the availability of alternate accelerator technologies, reduced activation and radiation hazard, reduced system size, and reduced shielding requirements.

The advantages of FEL operation with electromagnetic pump (wiggler) waves has led to the study of several novel configurations. One important and promising concept is that of the two stage FEL [11-15] in which a conventional magnetostatic wiggler produces an electromagnetic wave in the first stage, and this wave is then used as a pump wave utilizing the same electron beam in a second stage. In this paper, we present an analysis of an

FEL configuration which also utilizes two stages and an electromagnetic wiggler. However, the concept [16] discussed here differs from the concept discussed above in that separate electron beams are used for each stage, and a cyclotron resonance (gyrotron) interaction mechanism produces the wiggler electromagnetic field. The generation of an electromagnetic pump wave by a gyrotron requires only a low to moderate voltage electron beam, from fifty to a few hundred kV depending on the desired electromagnetic field strength. The electromagnetic wave produced by the gyrotron is then stored as an electromagnetic standing wave acting as the wiggler. We shall refer to this system as the Gyrotron powered Electro-Magnetic (GEM) wiggler. Although the gyrotron has been selected here as the prototype device for producing the electromagnetic wiggler field, most of the results for FEL gain obtained in this paper would also apply to EM wigglers produced by other high power sources of millimeter wave radiation.

The use of the gyrotron interaction for the first stage would benefit from recent progress in gyrotron oscillators. Gyrotrons are capable of routinely producing high power at high frequency (millimeter and submillimeter bands) with high efficiency [17,18]. A one megawatt, 140 GHz gyrotron is currently under development at MIT [17], and a 2 MW, 3 mm wavelength pulsed gyrotron has been demonstrated in the Soviet Union [18].

Alternatively, one could use relativistic cyclotron resonance devices, such as the relativistic gyrotron or the cyclotron autoresonance maser (also known as the wiggler free FEL)[19] to produce very high power electromagnetic pulses in the millimeter or submillimeter band. The power would propagate through the second stage FEL interaction region as a traveling wave in waveguide; the electromagnetic wiggler is then a traveling wave rather than a standing wave in a high Q cavity. The relativistic gyrotron has received considerable attention and several experiments have achieved impressive results, with 20 MW at 35 GHz and 8.5 percent efficiency achieved in one [20], and 23 MW at 40 GHz with 5 percent efficiency achieved in another [21]. Similarly, a cyclotron autoresonance maser has operated at 2.4 mm with 10 MW of power and 2 percent efficiency [22].

The use of high Q resonators for the wiggler field is appropriate for use with gyrotrons capable of long pulse operation. Gyrotrons with long pulse or CW capability employ thermionic cathodes. The high Q resonator is required to reach wiggler field

strengths high enough for reasonable FEL gain in the second stage. Alternatively, relativistic gyrotrons and cyclotron autoresonance masers produce significantly more peak power than do gyrotrons with thermionic cathodes, but, because they employ cold cathode technology, the pulse lengths are limited to less than approximately 100 ns. For these sources, propagation of the wiggler field as a traveling wave is more appropriate. In this paper, both traveling wave and standing wave resonator fields are considered as possible electromagnetic wigglers.

This paper is organized as follows. In section II, the gain for an FEL with an electromagnetic wiggler in the low and high gain Compton regimes is presented; the effects of e-beam emittance and transverse wiggler field inhomogeniety are discussed. The acceptance of the FEL with a TE_{1n} mode electromagnetic wiggler is derived. The gain scaling with beam brightness, number of wiggler periods, and current are discussed, and sample gain calculations are presented.

In section III, the wiggler field strength is calculated for two configurations, traveling wave TE_{1n} waveguide modes, and standing wave TE_{1nl} cavity modes. The dependence of the field strength on source power, mode, cavity configuration, wiggler wavelength and number of wiggler periods is discussed. In section IV, several configurations for an FEL with a GEM wiggler are proposed and discussed and conclusions are presented.

II. ELECTROMAGNETIC WIGGLER FEL GAIN

A. Low Gain Compton Regime

The gain for an FEL with an electromagnetic wiggler operating in the Compton regime is optimized in this section. The FEL resonance condition for a relativistic electron beam with energy γmc^2 $(U[MeV] = 0.511(\gamma - 1))$ propagating in an electromagnetic wiggler field of frequency $\omega = ck = 2\pi c/\lambda = c(k_\parallel^2 + k_\perp^2)^{1/2}$ is given by

$$k_s = 2\gamma^2 k_w (1 + a_w^2)^{-1} \tag{1}$$

where $k_w = k + k_\parallel$ and a_w is the normalized vector potential of the wiggler field, defined here by $a_w = eB_w/mc^2 k_\parallel$. Here $k = (k_\parallel^2 + k_\perp^2)^{1/2}$ is the wavenumber of the wiggler field with $k_\parallel$ and $k_\perp$ as its axial and transverse components. The inclusion of $k_\perp$ is necessary when considering electromagnetic wiggler fields in waveguides and resonant cavities, as is the case in this paper. The FEL gain is a strong function of a_w $(G \propto a_w^2)$; the calculation of reasonable values for a_w is deferred until the next section.

In the cold beam low gain Compton regime, the single pass gain expression [23,24] is given by

$$G_{cold} \equiv \frac{P(L) - P(0)}{P(0)},$$

$$G_{cold} = 1.77 \times 10^{-3} \frac{\lambda_s^{3/2} \lambda_w^{-5/2} I L^3 a_w^2 (1 + a_w^2)^{-3/2}}{A_b}, \tag{2}$$

where λ_w is the wavelength of the electron wiggle motion, given by $\lambda_w = \lambda/(1 + k_\parallel/k) = \lambda(1+\beta_{ph}^{-1})^{-1}$, where $\beta_{ph} = \omega/ck_\parallel$ is the phase velocity of the wiggler electromagnetic wave, and where I is the beam current in Amperes. In equation (2), A_b is the cross sectional area of the electron beam. Equation (2) applies to a beam with zero emittance, with zero transverse wiggler field inhomogeniety and filling factor of one (e-beam cross sectional area = radiation beam cross sectional area); hence we refer to it as the cold beam gain, G_{cold}. In order to include finite temperature effects we consider below the effect of finite emittance and transverse wiggler field inhomogeniety on the FEL resonance condition.

An electromagnetic wiggler produced from a gyrotron or cyclotron autoresonance maser is assumed to be in a TE_{1n} mode of a cylindrical waveguide or cavity. We consider

a circularly polarized traveling wiggler wave; the field dependence is given by the vector potential

$$\begin{aligned}\tilde{A}_w =& 2A_w\Big\{\frac{J_1(k_\perp r)}{k_\perp r}\left[\cos(k_\parallel z+\omega t)\cos\phi-\sin(k_\parallel z+\omega t)\sin\phi\right]\tilde{e}_r \\ &- J_1'(k_\perp r)\left[\cos(k_\parallel z+\omega t)\sin\phi+\sin(k_\parallel z+\omega t)\cos\phi\right]\tilde{e}_\phi\Big\},\end{aligned} \tag{3}$$

where $A_w = B_w/k_\parallel$, and B_w is the peak magnetic field on axis. $J_1(x)$ is a Bessel function and $k_\perp = \nu_{1n}/a$, where ν_{1n} is the n^{th} nonzero root of $J_1'(x) = 0$, and a is the waveguide radius. Near the axis, the vector potential can be approximated by

$$|\tilde{A}_w| = A_w\left(1-\frac{k_\perp^2 r^2}{8}\right). \tag{4}$$

The wiggler field is thus slightly defocusing. This is in contrast to the case of a magnetostatic wiggler in which the field varies in the transverse direction as either a hyperbolic cosine or a modified Bessel function with $|\tilde{A}_w| \simeq A_w(1+k_w^2 r^2/2)$ and is focusing. Although the electromagnetic wiggler is defocusing, the defocusing will be very weak because the field strength $a_w = eA_w/mc^2$ will generally be weak ($a_w^2 \ll 1$). An important difference between the waveguide electromagnetic (EM) wiggler and the conventional magnetostatic (MS) wiggler is that the transverse field variation depends on $k_\perp$ for the EM wiggler and not on k_w ($= k + k_\parallel$). Since $k_\perp$ can be made small by making the waveguide radius relatively large, the transverse inhomogeniety can in principle be small.

The effects of a transverse wiggler field inhomogeniety $k_\perp \neq 0$ and a finite emittance cause electrons in a nonideal electron beam to undergo different phase shifts in the FEL interaction region [25]. Because the energy transfer between the electron and optical mode is proportional to the vector dot product of the electron velocity and the electric field of the optical wave, the slowly varying phase for the FEL interaction is $\psi = k_w z + k_s z - \omega_s t$. In the low gain Compton regime net energy transfer over an interaction length L requires that the relative variation of ψ for any two electrons over the length L be less than some fraction of 2π radians. Choosing $\pi/2$ as the allowable relative phase variation [25], we can write

$$\left|\int_{-L/2}^{L/2} d\psi_1 - \int_{-L/2}^{L/2} d\psi_2\right| \leq \frac{\pi}{2}, \tag{5}$$

where the subscripts on ψ refer to electrons with different orbits. The equation of motion describing the evolution of ψ for a single electron can be shown to be [26]

$$\frac{d\psi}{dz} = k_w - \frac{k_s}{2\gamma^2}\left[1 + \langle\gamma^2\beta_\perp^2\rangle\right], \tag{6}$$

where $k_w = k + k_\parallel$ for the electromagnetic wiggler. The brackets $\langle\cdots\rangle$ denote an average over the wiggle period $2\pi/k_w$. Equation (5) can then be rewritten as

$$\left|\left[k_w - \frac{k_s}{2\gamma^2}\left(1 + \langle\gamma^2\beta_\perp^2\rangle\right)\right]_1 - \left[k_w - \frac{k_s}{2\gamma^2}\left(1 + \langle\gamma^2\beta_\perp^2\rangle\right)\right]_2\right| L \leq \frac{\pi}{2}. \tag{7}$$

At this point we consider electron orbits for the case of an electron beam for which the minimum beam radius occurs at the center of the interaction region, but for which there is no additional focusing within the FEL interaction. Axial guide fields [27] and quadrupole fields can allow beam transport over longer distances but are not considered here. The addition of focusing fields can have both beneficial and deleterious effects on the FEL resonance [28].

We consider one electron to have an orbit (orbit 1) described by:

$$x(z) = r_0\cos(k_w z) + r$$

$$y(z) = r_0\sin(k_w z)$$

where

$$r_0 = \frac{a_w}{\gamma k_w}\left(1 - \frac{k_\perp^2 r^2}{8}\right)$$

is the equilibrium radius of the helical wiggle motion. The second particle is assumed to pass through the interaction region at an angle given by the emittance $\epsilon \equiv rr'$ ($= (1/\pi)\times$ area in phase space) of the electron beam. For this particle, the orbit (orbit 2) is described by

$$x(z) = \frac{a_w}{\gamma k_w}\left(1 - \frac{k_\perp^2\epsilon^2}{8r^2}z^2\right)\cos(k_w z) + \frac{\epsilon}{r}z,$$

$$y(z) = \frac{a_w}{\gamma k_w}\left(1 - \frac{k_\perp^2\epsilon^2}{8r^2}z^2\right)\sin(k_w z).$$

Using $\beta_\perp^2 \simeq (dx/dz)^2 + (dy/dz)^2$, we can then evaluate $\langle\gamma^2\beta_\perp^2\rangle$ for both orbits. The result is

$$\langle\gamma^2\beta_\perp^2\rangle_1 = a_w^2\left(1 - \frac{k_\perp^2 r^2}{8}\right)^2, \tag{8a}$$

$$\langle\gamma^2\beta_\perp^2\rangle_2 = a_w^2 + \frac{\gamma^2\epsilon^2}{r^2} + a_w^2\left[\frac{2\pi^2}{3}b(2b-1) + \frac{\pi^4}{5}b^2\right], \tag{8b}$$

where $b = k_\perp^2 \epsilon^2 / 8 k_w^2 r^2$.

It is usually the case that $k_\perp^2 r^2 / 8 \ll 1$ and that the last term of the second expression is negligible. Then (8) becomes

$$\langle \gamma^2 \beta_\perp^2 \rangle_1 = a_w^2 \left(1 - \frac{k_\perp^2 r^2}{4} \right),$$

$$\langle \gamma^2 \beta_\perp^2 \rangle_2 = a_w^2 + \frac{\gamma^2 \epsilon^2}{r^2}.$$

Substitution of these expressions into Eq. (7) together with the FEL resonance condition (1) then result in a condition on the allowable emittance and wiggler inhomogeniety for the FEL;

$$\left| N a_w^2 k_\perp^2 r^2 + 4N \frac{\gamma^2 \epsilon^2}{r^2} \right| \leq 1, \tag{9}$$

where $N = L/\lambda_w$ is the number of electron oscillations in the wiggler, and where we have assumed $k_s \simeq 2\gamma^2 k_w, a_w^2 \ll 1$.

If equation (9) is written in terms of r and $\gamma r'$, one obtains the equation of an ellipse in $(r, \gamma r')$ phase space. The normalized acceptance of the GEM wiggler can then be defined as the product of the major and minor axes of the ellipse;

$$A_n = \gamma r r' = (2 N a_w k_\perp)^{-1}. \tag{10}$$

Provided the phase space of all the electrons in a beam is bounded by this ellipse at the center of the wiggler, all particles will suffer less than a $\pi/2$ relative phase shift. This is to be compared with the acceptance of a helical magnetostatic wiggler given by [25]; $A_n^{ms} = (2\sqrt{2} N a_w k_w)^{-1}$ in the limit of $a_w^2 \ll 1$.

An important difference between the electromagnetic wiggler and the magnetostatic wiggler is apparent from comparison of the acceptance in the two cases. For short wavelength wigglers and comparable a_w, the acceptance of the electromagnetic wiggler can be made significantly larger than the acceptance of a corresponding magnetostatic wiggler, because in the case of the EM wiggler, $k_\perp$ can be decreased significantly without significantly changing $k_w = k + k_\parallel$.

The effect of finite emittance and a transverse wiggler field inhomogeniety on the gain can be calculated by treating each as a thermal spread in the FEL detuning parameter.

Many authors have treated these effects in such a way for the case of the magnetostatic wiggler. We define [24,29] the synchronism detuning parameter θ as $\theta = \omega_s/v_{z0} - k_s - k_w$, the detuning thermal spread parameter as $\theta_{th} = \omega_s v_{z,th}/v_{z0}^2$, where v_{z0} is the axial velocity of the electron beam, and $v_{z,th}$ as the axial velocity spread of the electron beam. A normalized detuning spread parameter $\bar{\theta}_{th}$ is defined by $\bar{\theta}_{th} \equiv \theta_{th} L$. Then the finite emittance contributes a detuning spread given by

$$\bar{\theta}_{th,1} = 2\pi N \frac{\epsilon_n^2}{r_b^2}, \tag{11}$$

where r_b is the electron beam radius at the center of the wiggler, and $\epsilon_n \equiv \gamma\beta\epsilon$ is the normalized emittance. For $k_\perp = 0$, the acceptance criterion (9) can be written $\bar{\theta}_{th,1} \leq \pi/2$.

Similarly, the transverse wiggler field inhomogeniety contributes to a detuning spread

$$\bar{\theta}_{th,2} = \frac{\pi}{2} N a_w^2 k_\perp^2 r_b^2. \tag{12}$$

The total detuning spread is then given by $\bar{\theta}_{th}^2 = \bar{\theta}_{th,1}^2 + \bar{\theta}_{th,2}^2$.

Degradation of the cold beam gain due to finite $k_\perp$ and ϵ_n can be calculated numerically as a function of $\bar{\theta}_{th}$. However, for an electron beam in the intermediate cold-warm tenuous beam, low gain regime, Jerby and Gover [24] have shown that the numerically computed gain can be closely approximated by the expression

$$G(\bar{\theta}_{th}) = \frac{G_{cold}}{1 + \bar{\theta}_{th}^2/\pi^2}, \tag{13}$$

where the cold beam gain is given by Eq. (2).

The gain as given by Eq. (13) can be optimized for fixed I, N, and brightness $B_n \equiv I/\pi^2\epsilon_n^2$ with respect to the electron beam radius r_b. The resulting optimum radius is given by

$$r_{b,opt} = \frac{1}{a_w k_\perp} \left\{ \frac{2}{3N^2} \left[\sqrt{1 + 12(N\epsilon_n a_w k_\perp)^4} - 1 \right] \right\}^{\frac{1}{4}}, \tag{14}$$

or, for the case $12(N\epsilon_n a_w k_\perp)^4 \ll 1$, which usually holds,

$$r_{b,opt} \simeq (2N)^{1/2} \epsilon_n = \left(\frac{2NI}{\pi^2 B_n} \right)^{1/2}. \tag{15}$$

The optimum electron beam radius decreases as the number of periods and the current decrease and increases as the beam brightness decreases. A lower limit on r_b results from the diffraction of the optical beam and the concomitant reduction in FEL coupling to the optical mode [30]. This limit is $\pi r_{b,opt}^2 \geq \lambda_s L/2\sqrt{3}$, the minimum optical mode area. When this limit is violated by Eq. (14) or (15), we take

$$r_b = \left(\frac{\lambda_s \lambda_w N}{2\pi\sqrt{3}}\right)^{1/2}. \tag{16}$$

Two different gain scalings result from the two different expressions for the beam radius. For low currents,

$$I < I_1 \equiv \frac{\pi \lambda_s \lambda_w B_n}{4\sqrt{3}},$$

the optimized radius given by (15) results in an e-beam with an area less than the minimum optical mode area, and the beam area is set equal to the minimum optical mode area. The gain then scales linearly with the current, for small currents, and is given by Eq. (13) with (11), (12) and (16),

$$G = 1.77 \times 10^{-3} \frac{2\sqrt{3}\lambda_s^{1/2}\lambda_w^{-1/2} N^2 a_w^2 I}{\left[1 + (I/I_1)^2 + (\lambda_s \lambda_w/\pi)^2 (N a_w k_\perp)^4/48\right]}. \tag{17}$$

The second term in the denominator is $\bar{\theta}_{th,1}^2/\pi^2$ and the third term is $\bar{\theta}_{th,2}^2/\pi^2$, with (16) for r_b^2. The third term is usually negligible compared with the second. One can see from Eq. (17) that as I approaches I_1, the gain is saturated by the finite emittance as described by $\bar{\theta}_{th,1}$.

For $I > I_1$, the optimum beam radius is given by (14), and the gain is given by

$$G = 1.77 \times 10^{-3} \frac{\lambda_s^{3/2} \lambda_w^{1/2} N^3 a_w^2 I}{\pi r_{b,opt}^2 [1 + 4N^2(\epsilon_n/r_{b,opt})^4 + N^2(a_w k_\perp r_{b,opt})^4/4]}. \tag{18a}$$

When Eq. (14) can be approximated by Eq. (15), the gain can be approximated by

$$G = 1.77 \frac{\pi}{4} \lambda_s^{3/2} \lambda_w^{1/2} N^2 a_w^2 B_n, \tag{18b}$$

where B_n is in kA/cm^{2}rad^2. For currents above I_1, the small signal gain is independent of current and depends only on brightness. The gain described by (18b) is approximately half the cold beam gain at $r = r_{b,opt}$.

The small signal gain has been calculated as a function of current for several different values of the electromagnetic wiggler wavelength and beam brightness. A wiggler amplitude of $a_w = 0.05$ is assumed; this corresponds to a traveling wave with a magnetic field of approximately 0.5, 1, and 2.5 kG for $\lambda = 1$, 0.5, and 0.2 cm, respectively. Such a wiggler amplitude requires high power sources of electromagnetic radiation such as gyrotrons or other cyclotron resonance devices. A discussion of power requirements and possible configurations is deferred to the following sections.

Figures 1 through 3 show the gain versus current for several beam brightnesses. Brightnesses of 240 $\mathrm{kA/cm^2rad^2}$ and $1 \times 10^3\,\mathrm{kA/cm^2rad^2}$ are possible with present rf linacs and electrostatic accelerators [31]. A 2.5 MeV injector employing accelerator cells excited at the fundamental and harmonics has been proposed [32]; such a system is potentially capable of very high brightness. The use of photocathodes may also bring about large increases in brightness. The gain is also calculated assuming a brightness of $5 \times 10^3\,\mathrm{kA/cm^2rad^2}$.

The calculated FEL gain is shown in Fig. 1 for the case of a 30 GHz, $\lambda = 1$ cm gyrotron powered electromagnetic wiggler and a $\lambda_s = 10\,\mu$m FEL output wavelength. A 7.8 MeV electron beam would be required for $10\,\mu$m operation. The wiggler electromagnetic wave phase velocity is assumed to be $\beta_{ph}^{-1} = k_{||}/k = 0.9$ for all the following examples. The gain for two different brightnesses and for N=100 and N=200 wiggler periods is shown. The brightnesses are quoted in units of $\mathrm{kA/cm^2rad^2}$. For the 240 $\mathrm{kA/cm^2rad^2}$ brightness, the gain scaling changes from a linear dependence on current described by (17) to a constant gain independent of current for $I > I_1 = 57$ A. For higher brightness the transition between scaling laws occurs at higher currents. For both regimes, the gain scales as N^2.

The calculated gain for a 60 GHz gyrotron powered electromagnetic wiggler ($\lambda = 5\,$mm) is shown in Fig. 2 for three different brightness beams. The transition between the different gain scalings can be seen for the 240 $\mathrm{kA/cm^2rad^2}$ brightness, and the beginning of the transition can be seen for the $B_n = 240\,\mathrm{kA/cm^2rad^2}$, $N = 100$ case. In the region where gain scales linearly with current, different gain for different brightness beams at the same current results from the finite emittance corrections to the gain (Eq. 13). It is clear from Fig. 2 that for reasonable brightness, the gain for a $\lambda = 5\,$mm wiggler with $a_w = 0.05$, $\lambda_s = 10\,\mu$m, (5.35 MeV beam) is sufficient for FEL operation.

The gain for $\lambda = 2\,\mathrm{mm}$ electromagnetic wiggler is shown in Fig. 3. At this wiggler wavelength, only a 3.2 MeV beam is required for $\lambda_s = 10\,\mu\mathrm{m}$ operation. The decrease in gain with increase in current for the $B_n = 240\,\mathrm{kA/cm^2 rad^2}, N = 100$ and $N = 200$ cases is due to the current dependence in Eq. (18a).

It is clear from these figures that no appreciable improvement in gain is achieved by using electron beams which exceed the limiting current I_1. Thus, with all other parameters fixed, higher FEL gain requires higher quality beams with low emittance.

Because of the gain dependence on $(Na_w)^2$ for both (17) and (18), it appears attractive to increase N and decrease a_w by the same factor. Although the efficiency of the electromagnetic wiggler would decrease (efficiency $\sim 1/2N$), the FEL gain based on (17) or (18) would remain unchanged. The advantage would be a reduced a_w and hence a reduced electromagnetic power density required for reasonable FEL gain. For certain accelerator technologies this may prove practical. However, two additional effects could reduce this potential advantage. Pulse slippage and the finite energy spread contribution to $\bar{\theta}_{th}$ will set an upper limit on the degree to which this trade-off can be made for different accelerator technologies.

A slippage parameter $s \equiv N\lambda_s/c\tau_p$ can be defined for a given wiggler (N) and electron pulse temporal width τ_p. When s approaches unity, initially overlapping electron and optical pulses separate completely in transit through the wiggler, resulting in a considerable degradation of the gain (laser lethargy). For electrostatic and induction acclerators, τ_p is generally large and slippage is not an issue. For rf linacs, we require $s \leq s_0$, some maximum allowable value. For $\tau_p = \delta_r T_{rf}/2\pi$, where δ_r is the phase angle of the electron bunch in radians, and $T_{rf} = 1/f_{rf}$ is the rf accelerator period, the condition on s can be written $\delta_r^2 \geq 2\pi N\lambda_s f_{rf}/cs_0$.

The contribution to $\bar{\theta}_{th}$ from energy spread can be expressed as $\bar{\theta}_{th} \simeq 2\pi N\Delta\gamma/\gamma$ [24]. For a single frequency rf accelerator, $\Delta\gamma/\gamma \simeq \delta_r^2/8$, and, with a reasonable limit on this contribution to the detuning spread parameter, $\bar{\theta}_{th} \leq \pi/2$, this condition can be written $\delta_r^2 \leq 2/N$. The slippage problem worsens as δ_r decreases, but the energy spread problem worsens as δ_r increases. An estimate of the limit to N due to these two effects can be

obtained by combining these two conditions:

$$N \leq N_{lim} \equiv \left[\frac{\sqrt{2}}{2\pi}\frac{s_0 c}{f_{rf}\lambda_s}\right]^{2/3}.$$

For an rf linac with $f_{rf} \sim 500$ MHz, $s_0 \sim 0.2$, and $\lambda_s = 10\,\mu$m, $N_{lim} \simeq 200$ periods. Operation with higher frequency optical radiation reduces the slippage problem, but the energy spread requirements for any accelerator technology become more severe as N increases.

Although GEM wiggler FEL operation with conventional rf linear accelerators may be limited to wigglers of ~200 periods, rf linear accelerators employing higher order mode, harmonically excited cells [32] could lessen both these constraints on the maximum N. The operation of a GEM wiggler FEL with an electrostatic accelerator would avoid the slippage problem, but the constraint due to finite energy spread remains.

One final contribution to the detuning spread parameter which may become significant for very low voltage beams is due to space charge. This contribution is approximately [24]

$$\bar{\theta}_{th}|_{sc} \simeq 1.2\pi \times 10^{-4}\frac{NI}{\gamma},$$

where I is in amps. For N~200, I~100 A, and $\gamma \sim 10$, $\bar{\theta}_{th}|_{sc} \sim \pi/4$, and the space charge contribution to $\bar{\theta}$ may result in a small decrease in FEL gain. For larger N and smaller γ, this correction becomes more significant.

B. High Gain Compton Regime

The calculations discussed in subsection A refer to FELs with weak electromagnetic wiggler fields ($a_w \ll 1$) where the gains are low ($G < 1$). However, the high gain regime may well be reached using an intense electromagnetic wiggler. The computations in this section are appropriate to this mode of operation; the free electron laser stability properties have also been calculated in the high-gain Compton regime using a model based on the Vlasov-Maxwell equations. We consider a relativistic electron beam propagating in the positive z-direction through the backward-traveling, circularly-polarized electromagnetic wiggler with vector potential ($k_\parallel \simeq k$ in this discussion)

$$\tilde{A}_w(\tilde{x},t) = \frac{mc^2}{e}a_w\left[\cos(kz+\omega t)\tilde{e}_x - \sin(kz+\omega t)\tilde{e}_y\right], \tag{19}$$

where $a_w = eB_w/mc^2k$ = const. is the normalized wiggler amplitude. For present purposes, transverse spatial variations are neglected ($\partial/\partial x = 0 = \partial/\partial y$), and the electron beam is assumed to be sufficiently tenuous that longitudinal perturbations can be neglected (Compton-regime approximation with $\delta\phi \simeq 0$). Furthermore, we consider the class of self-consistent beam distribution functions of the form [33,34]

$$f_b(z,\tilde{p},t) = \hat{n}_b\,\delta(P_x)\,\delta(P_y)\,G(z,p_z,t), \tag{20}$$

where P_x and P_y are the exact transverse canonical momenta defined by $P_x = p_x - (e/c)A_{xw}(z,t) - (e/c)\delta A_x(z,t)$ and $P_y = p_y - (e/c)A_{yw}(z,t) - (e/c)\delta A_y(z,t)$. Here, $\tilde{p} = \gamma m\tilde{v}$ is the mechanical momentum, $\gamma = (1 + \tilde{p}^2/m^2c^2)^{1/2}$ is the relativistic mass factor, $\hat{n}_b$ = const. is the average electron density, and δA_x and δA_y are the transverse components of the perturbed vector potential. For the class of distribution functions in Eq. (20), note that the electrons move on surfaces with $P_x = 0 = P_y$ corresponding to zero transverse emittance. Moreover, it is readily shown that the one-dimensional distribution function $G(z,p_z,t)$ evolves according to the nonlinear Vlasov equation [33]

$$\left\{\frac{\partial}{\partial t} + v_z\frac{\partial}{\partial z} - mc^2\frac{\partial\gamma_T}{\partial z}\frac{\partial}{\partial p_z}\right\}G(z,p_z,t) = 0, \tag{21}$$

where $v_z = p_z/\gamma_T m$, and $\gamma_T(z,p_z,t)$ is defined by

$$\gamma_T = \left\{1 + \frac{p_z^2}{m^2c^2} + [a_w\cos(kz+\omega t) + \delta a_x]^2 + [-a_w\sin(kz+\omega t) + \delta a_y]^2\right\}^{1/2}. \tag{22}$$

Here, $\delta a_x = (e/mc^2)\,\delta A_x$ and $\delta a_y = (e/mc^2)\,\delta A_y$, and longitudinal perturbations have been neglected $\delta\phi \simeq 0$.

A detailed kinetic stability analysis [33] proceeds by expressing $G(z,p_z,t) = G_0(p_z) + \delta G(z,p_z,t)$ and solving the linearized Vlasov-Maxwell equations for $\delta G(z,p_z,t)$, $\delta a_x(z,t)$, and $\delta a_y(z,t)$. As an equilibrium constraint it is found that the wiggler frequency ω and wavenumber k are related self-consistently by

$$\omega^2 = c^2k^2 + \hat{\omega}_{pb}^2\int_{-\infty}^{+\infty}\frac{dp_z}{\gamma_0}G_0(p_z), \tag{23}$$

where $\hat{\omega}_{pb}^2 = 4\pi\hat{n}_b e^2/m$ is the nonrelativistic plasma frequency-squared, $G_0(p_z)$ is the equilibrium distribution function, and $\gamma_0 = \gamma_T(\delta a_x = 0, \delta a_y = 0)$ is the relativistic mass factor defined by

$$\gamma_0 = \left(1 + \frac{p_z^2}{m^2c^2} + a_w^2\right)^{1/2}. \tag{24}$$

We parallel the kinetic stability analysis given in [33] and orginally carried out for a static helical wiggler. Making the Compton-regime approximation and assuming electromagnetic perturbations with (nearly) right-circular polarization, the linearized Vlasov-Maxwell equations give the dispersion relation

$$\hat{\omega}^2 - c^2\hat{k}^2 - \hat{\alpha}\hat{\omega}_{pb}^2 = -\frac{1}{2}a_w^2\hat{\omega}_{pb}^2\int_0^\infty \frac{dp_z}{\gamma_0^2}\frac{(\hat{k}+k)v_z\,\partial G_0^+/\partial\gamma_0}{(\hat{\omega}-\omega)-(\hat{k}+k)v_z}. \tag{25}$$

Here, $v_z = p_z/\gamma_0 m$ is the axial velocity, $\hat{k}$ is the wavenumber of the perturbation, and $\hat{\omega}$ is the (complex) oscillation frequency with $Im\,\hat{\omega} > 0$ corresponding to temporal growth. Moreover, the normalization constant $\hat{\alpha}$ in Eq. (25) is defined by

$$\hat{\alpha} = \int_0^\infty \frac{dp_z}{\gamma_0}\left(1 - \frac{1}{2}\frac{a_w^2}{\gamma_0^2}\right)G_0^+(\gamma_0), \tag{26}$$

and we have assumed that the beam electrons are moving in the positive z- direction with

$$G_0(p_z) = U(p_z)G_0^+(\gamma_0). \tag{27}$$

In Eq. (27), $U(p_z)$ is the Heaviside function defined by $U(p_z) = 1$ for $p_z > 0$ and $U(p_z) = 0$ for $p_z < 0$. For future reference, it is straightforward to show from Eq. (24) that the axial velocity $\beta_z c = v_z$ can be expressed as

$$\beta_z^2 = 1 - \frac{1 + a_w^2}{\gamma_0^2}. \tag{28}$$

The Compton-regime dispersion relation (25) can be used to investigate detailed kinetic stability properties over a wide range of system parameters and choice of distribution functions $G_0^+(\gamma_0)$. In the regime of practical interest, we assume that the electron beam is sufficiently tenuous that

$$\hat{\alpha}\hat{\omega}_{pb}^2 \ll c^2\hat{k}^2. \tag{29}$$

In addition, it is assumed that the distribution of beam electrons $G_0^+(\gamma_0)$ is strongly peaked about average energy $\gamma_0 = \gamma_b$ with (small) energy spread $\Delta\gamma_0$ satisfying

$$\Delta\gamma_0 \ll \gamma_b. \tag{30}$$

The FEL growth rate generally exhibits a sensitive dependence on the detailed form of $G_0^+(\gamma_0)$ even when the inequality in Eq. (30) is satisfied.

FEL Resonance Conditions : Within the context of (29) and (30), the dispersion relation (25) exhibits strong FEL coupling for frequency and wavenumber $(\hat{\omega}, \hat{k}) = (\omega_s, k_s)$ satisfying the simultaneous resonance conditions

$$\begin{aligned} \omega_s &= ck_s, \\ \omega_s &= \omega + (k_s + k)V_b. \end{aligned} \tag{31}$$

Here, the average beam velocity $V_b = \beta_b c$ is defined by $c\beta_b = [1-(1+a_w^2)/\gamma_b^2]^{1/2}c$. Solving Eq. (31) for k_s gives $ck_s = (1 - V_b/c)^{-1}(\omega + kV_b)$, or equivalently,

$$k_s = \frac{\gamma_b^2}{1+a_w^2}(1+\beta_b)(\omega/kc + \beta_b)k. \tag{32}$$

If further it is assumed that $c^2k^2 \gg \hat{\omega}_{pb}^2 \int_0^\infty dp_z G_0^+/\gamma_0$, then $\omega = ck$ is a good approximation to Eq. (23), and the characteristic wavenumber k_s of the FEL radiation can be expressed as

$$k_s = \frac{\gamma_b^2}{1+a_w^2}(1+\beta_b)^2 k. \tag{33}$$

For relativistic electrons, $\beta_b \simeq 1$ and Eq. (33) is equivalent to Eq. (1).

Strong FEL Instability – Monoenergetic Electrons : As a first application of the kinetic dispersion relation (25), we consider the case where the energy spread $\Delta\gamma_0$ is sufficiently small that $|\hat{k}+k|\Delta v_z \ll |\hat{\omega}-\omega|$. Here, Δv_z is the axial velocity spread characteristic of $G_0^+(\gamma_0)$, and Δv_z is related to the energy spread $\Delta\gamma_0$ by $\Delta v_z = c[(1+a_w^2)/\gamma_b^3](c/V_b)\Delta\gamma_0$. For sufficiently small $\Delta\gamma_0$, it is valid to approximate $G_0^+(\gamma_0)$ by (Fig. 4a)

$$G_0^+(\gamma_0) = \frac{V_b}{mc^2}\,\delta(\gamma_0 - \gamma_b), \tag{34}$$

where the normalization condition is $\int_0^\infty dp_z\, G_0^+(\gamma_0) = 1$. Substituting Eq. (34) into the dispersion relation (25) readily gives

$$\hat{\omega}^2 - c^2\hat{k}^2 - \hat{\alpha}\hat{\omega}_{pb}^2 = \frac{1}{2}a_w^2\hat{\omega}_{pb}^2\left[\frac{(1+a_w^2)}{\gamma_b^5}\frac{c^2(\hat{k}+k)^2}{[(\hat{\omega}-\omega)-(\hat{k}+k)V_b]^2} - \frac{2}{\gamma_b^3}\frac{(\hat{k}+k)V_b}{[(\hat{\omega}-\omega)-(\hat{k}+k)V_b]}\right], \tag{35}$$

where $V_b = c[1-(1+a_w^2)/\gamma_b^2]^{1/2}$. The dispersion relation (35), valid for monoenergetic electrons, can be solved for the growth rate $Im\,\hat{\omega}$ over a wide range of system parameters. For present purposes, we assume $\hat{\alpha}\hat{\omega}_{pb}^2 \ll c^2\hat{k}^2$, and express $\hat{\omega} = \omega_s + \delta\omega_s$ and $\hat{k} = k_s + \delta k_s$, where ω_s and k_s solve Eq. (31). Retaining the dominant contribution proportional to $[(\hat{\omega}-\omega)-(\hat{k}+k)V_b]^{-2}$ on the right-hand side of Eq. (35), the characteristic maximum growth rate is determined from

$$2\omega_s(\delta\omega_s)^3 = \frac{1}{2}a_w^2\hat{\omega}_{pb}^2\frac{(1+a_w^2)c^2(k_s+k)^2}{\gamma_b^5} \tag{36}$$

for $\delta k_s = 0$ and $|\delta\omega_s| \ll \omega_s$. We make use of Eq. (33) to eliminate $k_s + k$ in Eq. (36) in favor of k. Solving for $Im\,(\delta\omega_s)$ then gives the characteristic growth rate

$$Im\,(\delta\omega_s) = \frac{\sqrt{3}}{2}\left(\frac{a_w^2\hat{\omega}_{pb}^2 ck}{\gamma_b^3}\right)^{1/3}. \tag{37}$$

Because an ideal electron beam (monoenergetic electrons) has been assumed, the growth rate in Eq. (37) corresponds to the largest growth rate achievable in the high-gain Compton-regime.

Weak Resonant FEL Growth : Kinetic stability properties are altered significantly when the energy spread in the beam electrons is sufficiently large that $|\hat{k}+k|\,\Delta v_z \gg |Im\,\hat{\omega}|$ (Fig. 4b). In this case, resonant electrons play the controlling role in determining the instability growth rate. For $\hat{\alpha}\hat{\omega}_{pb}^2 \ll c^2\hat{k}^2$ and $|Im\,\hat{\omega}| \ll |\hat{k}+k|\,\Delta v_z$, it is readily shown from Eq. (35) that the growth rate is given by

$$Im\,\omega_s = \frac{\pi}{4}\frac{a_w^2}{1+a_w^2}\frac{\hat{\omega}_{pb}^2}{\omega_r}\frac{(\hat{k}+k)}{|\hat{k}+k|}\left[p_z\frac{\partial G_0^+}{\partial\gamma_0}\right]_{\gamma_0=\hat{\gamma}_r}. \tag{38}$$

Here, the resonant energy $\hat{\gamma}_r$ is defined by $\hat{\gamma}_r = (1 + \hat{p}_r^2/m^2c^2 + a_w^2)^{1/2}$, where $\hat{p}_r = \hat{\gamma}_r m \hat{v}_r$, and the resonant axial velocity $\hat{v}_r$ is defined by

$$\hat{v}_r = \frac{\omega_r - \omega}{\hat{k} + k}. \tag{39}$$

Combining Eq. (39) with the definition of $\hat{\gamma}_r$ also gives

$$\hat{\gamma}_r^2 = (1 + a_w^2)\left[1 - \left(\frac{\omega_r - \omega}{\hat{k} + k}\right)^2 \frac{1}{c^2}\right]^{-1}. \tag{40}$$

In Eqs. (39) and (40), $\omega_r = Re\,\hat{\omega} \simeq c\hat{k}$ for $\hat{\alpha}\hat{\omega}_{pb}^2 \ll c^2\hat{k}^2$. Note from Eq. (38) that the growth rate $Im\,\hat{\omega}$ depends on the detailed form of $G_0^+(\gamma_0)$ in the resonant region where $v_z = v_r = (\omega_r - \omega)/(\hat{k} + k)$.

As a particular example, we consider the case where the electrons have a Gaussian distribution in energy with $G_0^+(\gamma_0) = \text{const.} \times \exp[-(\gamma_0 - \gamma_b)^2/2(\Delta\gamma_0)^2]$, where $\gamma_b = \text{const.}$ is the average energy, and $\Delta\gamma_0 = \text{const.}$ is the energy spread. It is readily shown from Eq. (38) that the maximum growth rate occurs for $\gamma_r - \gamma_b = -\Delta\gamma_0$ with

$$\frac{(Im\,\hat{\omega})_{MAX}}{ck} = \frac{1}{4}\left(\frac{\pi}{e}\right)^{1/2} \frac{a_w^2}{\gamma_b^3} \frac{\hat{\omega}_{pb}^2}{c^2k^2} \frac{\beta_b^2}{(1 + \beta_b)^2} \left(\frac{\gamma_b}{\Delta\gamma_0}\right)^2. \tag{41}$$

Here, $(\pi/e)^{1/2} = 1.075$ and $\beta_b^2 = 1 - (1 + a_w^2)/\gamma_b^2$. For sufficiently large energy spread, as shown in [35] for the case of a static magnetic wiggler, the growth rate in Eq. (38) can be substantially less [36] than the ideal growth rate for monoenergetic electrons in Eq. (37). That is, beam quality (as measured by $\Delta\gamma_0/\gamma_b$) can have a large influence on detailed FEL stability behavior in the high gain Compton regime.

The critical energy spread $(\Delta\gamma_0/\gamma_b)_{cr}$ for the transition to the weak resonant FEL instability is readily calculated from $(Im\,\hat{\omega})_{MAX} = (k_s + k)\Delta v_z$, where $\Delta v_z = c[(1 + a_w^2)/\gamma_b^3](c/V_b)\Delta\gamma_0$. Making use of Eq. (41), we find

$$\left(\frac{\Delta\gamma_0}{\gamma_b}\right)_{cr} = 0.512 \frac{\beta_b}{1 + \beta_b} \left(\frac{a_w^2}{\gamma_b^3} \frac{\hat{\omega}_{pb}^2}{c^2k^2}\right)^{1/3}. \tag{42}$$

For a narrow energy spread with $\Delta\gamma_0/\gamma_b \ll (\Delta\gamma_0/\gamma_b)_{cr}$, the dispersion relation (35), derived for monoenergetic electrons, gives an excellent description of FEL stability properties. On the other hand, for sufficiently large energy spread that $\Delta\gamma_0/\gamma_b \gg (\Delta\gamma_0/\gamma_b)_{cr}$,

the (weak) growth rate is given by the resonant expression in Eq. (38). For parameters $a_w \sim 0.5$, $I/A_b = 3.3\,\mathrm{kA/cm^2}$, $\gamma_b \sim 10$, and $\omega/2\pi \sim 60\,\mathrm{GHz}$, equation (42) gives $(\Delta\gamma_0/\gamma_b)_{cr} \sim 0.005$. Because the energy spread for typical accelerators [31] is likely to be comparable to or larger than $(\Delta\gamma_0/\gamma_b)_{cr}$, the growth rate in the high gain regime should be calculated from Eq. (38).

C. Effect of Wiggler Field Forward Wave

In the preceeding discussion we have considered an electromagnetic traveling wave (3) as the wiggler field. It is also possible, and perhaps desirable, to use an electromagnetic standing wave in a high Q resonator. High values of a_w may be obtained by storage of the gyrotron power in a single high Q cavity mode. The resulting standing wave wiggler field can be written as the sum of two oppositely directed traveling waves of equal amplitude. Near the z-axis, the field can be written as

$$\tilde{A}_w(z,t) = A_w\big(\tilde{e}_x\cos(k_\parallel z+\omega t) - \tilde{e}_y\sin(k_\parallel z+\omega t) + \tilde{e}_x\cos(k_\parallel z-\omega t) + \tilde{e}_y\sin(k_\parallel z-\omega t)\big).$$

For an electron beam propagating in the $\tilde{e}_z$ direction, the backward traveling wave component produces the fast wiggle motion of the electron beam with a wave number of $k_w^+ = k/\beta_\parallel + k_\parallel$. In a standing wave field, the forward wave component of the wiggler field also produces a wiggle motion on the electron beam with a wavenumber of $k_w^- = k/\beta_\parallel - k_\parallel$. The equilibrium radius of the fast time scale helical motion due to the backward wiggler wave is $r = a_w/\gamma k_w^+$. The radius of the electron guiding center helical motion due to the forward wave is given by

$$R = \frac{a_w}{\gamma k_w^-} = \frac{a_w}{\gamma k}\left[\frac{1}{1-(k_\parallel/k)+\gamma^{-2}}\right].$$

For $k_\parallel \to k$, $R \to a_w\gamma/k$, and the guiding center helical motion of a single electron may be comparable to the electron beam radius. In this case, the detuning parameter spread may be significantly modified, and the deleterious effect of finite $k_\perp$ will be more severe. For $k_\parallel/k < 1$, the radius for the guiding center helical orbit of a single electron becomes much smaller than typical electron beam radii, so that the preceeding treatment for a

circularly polarized traveling wave adequately describes the circularly polarized standing wave wiggler.

Operation with a standing wave electromagnetic wiggler results in two separate FEL resonances with resonance conditions $k_s = 2\gamma^2(k \pm k_\parallel)(1 + 2a_w^2)^{-1}$. These two resonances correspond to the two separate components of the motion due to the forward and backward waves. In the design of the high Q wiggler cavity and the laser optical cavity, care must be taken to prevent oscillation at the low frequency FEL resonance. A detailed analysis of the gain for the standing wave electromagnetic wiggler and the phenomenon of detrapping in the limit $k_\parallel/k \ll 1$ have been investigated and will be presented elsewhere.

D. Pump Depletion

The amount of depletion of wiggler or pump wave power by the generated optical wave can be estimated by considering the quantum picture of electrons Compton scattering pump photons into the optical wave. The ratio of the power loss by the wiggler, P_w, to the optical power produced by the FEL interaction, P_s is $P_w/P_s \simeq \omega/\omega_s \simeq 1/4\gamma^2$. For moderate γ, the average pump power depletion is a small fraction of the average optical power generated. Furthermore, gyrotrons are capable of high average power operation, so pump depletion is unlikely to pose a significant constraint on FEL performance. Pump depletion will be more important for FEL operation in the collective regime with high current beams.

The gain for gyrotron powered electromagnetic wigglers has been shown to be sufficient for FEL oscillator operation with modest current electron beams. The electromagnetic power required to produce the wiggler field strengths sufficient for high gain is discussed in the following section.

III. GEM Wiggler Field Strength

The feasibility of a gyrotron powered electromagnetic wiggler for FEL applications will depend not only on the available beam current, brightness, and number of wiggler periods, but also on the attainable wiggler field strength, a_w. The FEL gain scales as a_w^2; it is therefore important to determine the scaling of a_w with source power, frequency, cavity Q, and wiggler cavity mode. This scaling is addressed in this section for the cases of traveling wave propagation in waveguides and standing waves in high Q resonators.

For a traveling wave electromagnetic wiggler, we consider a TE_{1n} cylindrical waveguide mode. The TE_{1n} modes have fields on the axis that can be approximated by plane waves. Such modes are well suited for use as wigglers with high voltage axial electron beams. Furthermore, high power gyrotrons can produce significant power in these modes. For a power P flowing in a circular waveguide of radius a, the peak magnetic field on axis, B_w, can be related to P by [37]

$$B_w = \frac{\mu_0}{(\pi Z_0)^{1/2}} \left[(\nu_{1n}^2 - 1)J_1^2(\nu_{1n})\right]^{-1/2} k_\perp \sqrt{\frac{k_\parallel}{k}} \sqrt{P}, \tag{43}$$

where $k_\perp = \nu_{1n}/a$, and ν_{1n} is the n^{th} nonzero root of $J_1'(x) = 0$. For P in [MW] and wavenumbers in [cm^{-1}], the field in [kG] can be expressed as

$$B_w = 3.65 \times 10^{-2} \left[(\nu_{1n}^2 - 1)J_1^2(\nu_{1n})\right]^{-1/2} k_\perp \sqrt{k_\parallel/k} \sqrt{P}$$

for an arbitrary TE_{1n} mode. For propagation in a TE_{11} mode, the Bessel function factor $[\cdots]^{-1/2} = 1.11$, and $B_w = 4.06 \times 10^{-2}\, k_\perp \sqrt{k_\parallel/k} \sqrt{P}$. For fixed power and fixed $k_\perp$, B_w decreases slowly with higher order modes $TE_{1n}, n > 1$. The normalized vector potential for the circularly polarized traveling wave is then related to power by

$$a_w = 2.14 \times 10^{-2} \left[(\nu_{1n}^2 - 1)J_1^2(\nu_{1n})\right]^{-1/2} \frac{k_\perp}{\sqrt{k_\parallel k}} \sqrt{P\,[MW]}. \tag{44}$$

The normalized vector potential increases with $P^{1/2}$ and $k_\perp$. The FEL cold beam gain is thus proportional to $Pk_\perp^2$. However, Eq. (10) indicates that the acceptance decreases with increasing $k_\perp$. Thus the gain given by Eq. (13) will have an optimum with respect to $k_\perp$.

If this optimum occurs too close to cutoff ($k_{\|} \ll k$), other problems such as large ohmic loss may arise.

High power pulsed gyrotrons and cyclotron autoresonance masers ($P \sim 10 - 100\,\mathrm{MW}$) are thus capable of producing reasonable a_w values in circular TE_{1n} waveguide modes. As an example, consider a power $P = 20\,\mathrm{MW}$ at $\lambda = 5\,\mathrm{mm}$ propagating in a TE_{12} mode ($\nu_{12} = 5.33$) in waveguide of radius $a = 0.5\,\mathrm{cm}$. Then $k_{\perp} = 10.66\,\mathrm{cm}^{-1}$, $k_{\|} = 6.65\,\mathrm{cm}^{-1}$, and the magnetic field and vector potential are $B_w = 0.7\,\mathrm{kG}$ and $a_w = 0.062$. For power in the range of 10-100 MW, the vector potential ranges from $a_w \sim 0.04 - 0.14$.

Alternatively, the wiggler field can be stored in a high Q cavity. For a TE_{1nl} cavity mode in a right circular cylinder, the time averaged stored energy, W, can be written as

$$W = \frac{2\pi}{\mu_0}\left[(\nu_{1n}^2 - 1)J_1^2(\nu_{1n})\right]\left(\frac{k}{k_{\|}k_{\perp}}\right)^2 d\,B_w^2, \tag{45}$$

where $B_w = A_w/k_{\|}$ is the magnetic field strength of one of the traveling wave components of the standing wave and where d is the length of the cavity ($d \geq L$, the length of the FEL interaction). The equilibrium fields in the cavity can be obtained by equating the supplied power from the gyrotron, P_g, to the total time average dissipated power, P_d. The total Q of the system can be written $Q_T = \omega W/P_d$. At equilibrium, $P_g = P_d$, the field can be expressed as

$$B_w = 4.47 \times 10^3 \left[(\nu_{1n}^2 - 1)J_1^2(\nu_{1n})\right]^{-1/2} \frac{k_{\|}k_{\perp}}{k}\left(\frac{Q_T P_g}{\omega d}\right)^{1/2}, \tag{46}$$

where P_g is in [MW], lengths are in [cm] and B is in [kG]. The normalized vector potential can then be expressed as

$$a_w = 2.62 \times 10^3 \left[(\nu_{1n}^2 - 1)J_1^2(\nu_{1n})\right]^{-1/2} \frac{k_{\perp}}{k}\left(\frac{Q_T P_g}{\omega d}\right)^{1/2}. \tag{47}$$

The use of high Q cavities can allow high a_w for moderate power. The total Q is related to the cavity Ohmic Q, Q_{OHM} and any external or diffractive Q, Q_D, by $Q_T^{-1} = Q_{OHM}^{-1} + Q_D^{-1}$. The upper limit on Q_T is Q_{OHM}. Furthermore, P_g is the power supplied to the wiggler cavity and not necessarily the total power produced by the source. The degree to which the source power equals P_g and $Q_T \simeq Q_{OHM}$ will depend in a detailed way on the system configuration.

As an example of typical cavity parameters, we consider a high Q cylindrical cavity with $Q_T = Q_{OHM}/2$ and a $\lambda = 5\,\mathrm{mm}$ electromagnetic wiggler ($k_\parallel/k \simeq 1$). For a TE_{13} cavity mode with $N = 200$ periods in a cavity of radius $a = 1.56\,\mathrm{cm}$, the resulting field strength is $a_w = 4.2 \times 10^{-2}\sqrt{P_g\,[\mathrm{MW}]}$. For a dissipated power of $P_g = 1\,\mathrm{MW}$, $a_w = 0.042$, and $B_w = 0.9\,\mathrm{kG}$.

Several practical considerations may provide an upper limit to the attainable B_w and a_w for an EM wiggler. Surface breakdown does not appear to be a limitation at the wiggler field strengths necessary for reasonable FEL gain [38]. In high average power systems, ohmic heating of the wiggler resonator walls may require active cooling, but in FELs with modest pulse repetition rates this does not appear to be a problem. One problem that may prove important in high Q cavities is conversion of the stored power into unwanted modes by imperfections or tapers in the cavity. This may require mode supression techniques. Phase jitter in an EM wiggler system could also be a problem.

IV. Discussion and Conclusions

As an illustration of the advantages of an electromagnetic (EM) wiggler over a conventional magnetostatic (MS) wiggler for short wiggler wavelength and low beam voltage operation, the gain for both types of wigglers with comparable parameters is depicted in Fig. 5. An output wavelength of $\lambda_s = 10\,\mu$m is assumed, and the brightness, current, and number of wiggler periods are taken to be $B_n = 240\,\mathrm{kA/cm^2 rad^2}$, $I = 100\,\mathrm{A}$, and $N = 200$ for both cases. The beam voltage U required to produce $\lambda_s = 10\,\mu$m radiation is also shown. The EM wiggler field strength is assumed to be constant with $a_w = 0.05$, and we have assumed $k_\parallel/k = 0.9$ $(\lambda_w = \lambda/1.9)$. The magnetostatic wiggler is assumed to have a gap fixed at 7 mm, and the field is calculated from the usual expression [39] for a hybrid undulator. For the EM wiggler the gain is calculated from the full expression (Eqs. (17), (18)), including the effects of finite emittance and wiggler field inhomogeneity. The gain for the magnetostatic wiggler has been calculated assuming the optimization of reference [25], and with $\bar{\theta}_{th} = \pi/2$, as used in [25]. The gain is shown as a dashed line for gains above unity because the low gain expressions were used to calculate the gain.

For short wavelength wigglers, $\lambda_w < 1.5\,\mathrm{cm}$, the electromagnetic wiggler produces substantially more gain than the conventional hybrid undulator. At wiggler periodicities larger than 1.5 cm for these parameters, the magnetostatic wiggler will have higher gain and will be more attractive. Smaller gaps for the magnetostatic undulator will shift the MS gain curve in Fig. 5 to the left, but the GEM wiggler will maintain higher gain at short wavelengths. Of course, marked improvements in permanent magnet materials or the development of other short wavelength wigglers [40] could produce fields comparable to those of EM wave wigglers. Nevertheless, millimeter wavelength electromagnetic wigglers powered by gyrotrons or other cyclotron resonance devices appear promising.

Microwave undulators have been used for the generation of synchrotron radiation in the visible region of the spectrum using high voltage electron beams [41]; in this paper we are interested in the application of high frequency (millimeter wave) electromagnetic wigglers to free electron lasers. There are several possible configurations for FELs with gyrotron powered electromagnetic wigglers. The wiggler fields may be stored in a high

Q cavity or they may be traveling waves in waveguide or free space. In the case of a standing wave GEM wiggler in a cavity, several possibilities exist. The power source may be separated from the wiggler cavity, with external coupling into the cavity. High power microwave or millimeter wave circulators or isolators would be necessary to prevent reflection of power back to the source. Although these components may be feasible for lower frequency GEM wigglers ($\lambda \sim 0.5 - 1$ cm), higher frequency wigglers are likely to require an alternate concept.

One possible configuration is shown in Fig. 6. The gyrotron interaction and the FEL interaction take place in the same closed cavity. The gyrotron interaction occurs in the region of the cavity where $k_\perp \simeq k$ and where there is the axial magnetic field necessary for the interaction. The radiation produced in the gyrotron section is trapped inside the high Q cavity. The FEL interaction then occurs in a region of the high Q cavity in which $k_\perp < k$. The same mode produced in the gyrotron section of the cavity acts as the wiggler. The high voltage beam for the FEL interaction can be brought into the cavity through tapered openings in the cavity which are cutoff to the trapped mode or through slots in the resonator walls. The operation of gyrotrons in TE_{1n} modes with slotted resonators can be advantageous in terms of mode descrimination in the gyrotron interaction region. Alternatively, the high voltage beam may exit through a hole in the electron gun providing the beam for the gyrotron interaction; gyrotron electron guns are axisymmetric with the emitter strip located off axis by several centimeters. The optical resonator for the radiation produced by the FEL interaction may be axisymmetric and located as shown in Fig. 6.

The generation of a few megawatts of power by the gyrotron in Fig. 6 could produce wiggler field amplitudes sufficient for FEL oscillator operation. The high field strengths in the gyrotron interaction region would require operation of the gyrotron with short interaction lengths [18,42]; this is typical for high power gyrotrons.

A quasioptical gyrotron [43] or gyroklystron operating with a ring resonator could also be employed. A cyclotron autoresonance maser (CARM) could operate as the wiggler power source in either an optical resonator or a Bragg resonator [44].

In an alternate configuration for an electromagnetic wiggler, the wiggler field could be a traveling wave produced by a gyrotron or CARM. Higher peak powers would be

required than in the case of the high Q cavity, but the coupling problems are nonexistent. The temporal duration of the wiggler pulse constitutes a limitation of this configuration. If field emission cathodes are used, the wiggler electromagnetic pulse will be limited by gap closure. The FEL gain must then be sufficiently high to reach saturation during the wiggler pulse. For the high Q cavity configuration with a thermionic cathode, much longer duration (μs - CW) wiggler fields could be produced.

An infrared FEL system could be made extremely compact if the gyrotron which powered the electromagnetic wiggler was also used to power the electron accelerator. Part of the gyrotron output could be used to power a cyclotron resonance accelerator [45-47]. The resulting system could be quite compact with one high power gyrotron providing both the accelerating and wiggler fields.

The use of high current ($> 1\,\mathrm{kA}$) high brightness beams with short wavelength electromagnetic wigglers is also possible. Larger EM wiggler powers may be realistic in this case because the required EM wiggler power would still be small compared to the electron beam power.

Operation of an FEL with a GEM wiggler does not preclude efficiency enhancement schemes. As in the case of a magnetostatic wiggler, the GEM wiggler can be tapered. By varying the waveguide wall radius, $a(z) = \nu_{1n}/k_{\perp}(z)$, the wiggler wave number $k_w(z) = k + k_{\|}(z)$ and the field strength on axis may be tapered. For free space electromagnetic wigglers, no such controlled tapering is possible.

Other novel efficiency enhancement schemes are also possible. A compound wiggler consisting of a relatively long wavelength untapered EM wiggler and a strongly tapered magnetostatic wiggler could allow high efficiency FEL operation. Initially, at the start of the high voltage electron beam macropulse, the EM wiggler would provide high gain. As the optical field approaches saturation, the gyrotron powering the EM wiggler could be turned off, allowing the EM wiggler field to decay. The only remaining wiggler field is then due to the tapered magnetostatic wiggler. The extraction efficiency of the magnetostatic wiggler in the presence of a strong optical field can then be very high.

In conclusion, the recent considerable progress made in high power gyrotrons and other cyclotron resonance devices can have important implications for free electron lasers. The

operation of an FEL with short wavelength gyrotron powered electromagnetic wigglers can yield a significant reduction in the electron beam energy required to produce a given optical frequency. Such a considerable reduction in beam energy would result in more compact FEL systems with reduced activation and radiation shielding problems. Advantages of the GEM wiggler over the two-stage FEL include the high stability of gyrotron operation and efficient generation of the wiggler field by a separate low voltage electron beam.

The gain in the low and high gain Compton regime has been presented, and nonideal effects such as finite emittance, finite wiggler transverse gradient, energy spread, and pulse slippage have been discussed. Reasonable gains ($\sim 20-80\%$) are found for electron beams with a brightness obtainable from present day accelerators. Requirements on gyrotron power were obtained, and several possible GEM wiggler FEL configurations were suggested. The gyrotron powered electromagnetic wiggler appears promising for compact infrared free electron lasers.

Acknowledgements

The authors are grateful to G. Johnston, K. Kreischer, and N. Tishby for helpful discussions. This work was supported by the Department of Energy, the National Science Foundation, the Air Force Office of Scientific Research, and the Office of Naval Research. One of the authors (T.M.T.) would like to acknowledge the support received from the Swiss National Science Foundation.

REFERENCES

[1] D.A.G. Deacon, L.R. Elias, J.M.J. Madey, G.J. Ramian, H.A. Schwettman, and T.I. Smith, "First operation of a free-electron laser," Phys. Rev. Lett. 38, 892-894 (1977).

[2] J.A. Edighoffer, G.R. Neil, C.E. Hess, T.I. Smith, S.W. Fornaca and H.A. Schwettman, "Variable wiggler free electron laser oscillation," Phys. Rev. Lett. 52, 344-347 (1984).

[3] M. Billardon, P. Elleaume, J.M. Ortega, C. Baxin, M. Bergher, M. Velghe, Y. Petroff, D.A. G. Deacon, K.E. Robinson and J.M.J. Madey, "First operation of a storage ring free electron laser," Phys. Rev. Lett. 51, 1652-1655 (1983).

[4] T.J. Orzechowski, B. Anderson, W.M. Fawley, D. Prosnitz, E.T. Scharlemann, S. Yarema, D.B. Hopkins, A.C. Paul, A.M. Sessler and J. Wurtele, "Microwave radiation from a high-gain free electron laser amplifier," Phys. Rev. Lett. 54, 889-892 (1985).

[5] B.E. Newman, R.W. Warren, R.L. Sheffield, W.E. Stein, M.T. Lynch, J.S. Fraser, J.C. Goldstein, J.E. Sollid, T.A. Swann, J.M. Watson and C.A. Brau, "Optical performance of the Los Alamos free electron laser," IEEE J. Quantum Electron., QE-21, 867-881 (1985).

[6] L.R. Elias, "A submillimeter free electron laser," in Proc. 9th Int. Conf. Infrared and Millimeter Waves, Takarazuka, Japan, October 22-26, 1984, pp. 1-3.

[7] V.L. Granatstein, S.P. Schlesinger, M. Herndon, R.K. Parker and J.A. Pasour, "Production of megawatt submillimeter pulses by stimulated magneto Raman scattering," Appl. Phys. Lett. 30, 384-386 (1977).

[8] J.A. Pasour, R.F. Lucey and C.A. Kapetanakos, "Long pulse, high power, free electron laser with no external beam focusing," Phys. Rev. Lett. 53, 1728-1731 (1984).

[9] R.H. Jackson, S.H. Gold, R.K. Parker, H.P. Freund, P.C. Efthimion, V.L. Granatstein, M. Herndon, A.K. Kinkead, J.E. Kosakowski and T.J.T. Kwan, "Design and operation of a collective millimeter wave free electron laser," IEEE J. Quantum Electron., QE-19, 346-356 (1983).

[10] J. Fajans, G. Bekefi, Y.Z. Yin and B. Lax, "Spectral measurements from a tunable, Raman, free electron laser," Phys. Rev. Lett. 53, 246-249 (1984), and J. Fajans, G. Bekefi, Y.Z. Yin, and B. Lax, "Microwave studies of a tunable free electron laser in combined axial and wiggler magnetic fields", Phys. Fluids, 28, 1995-2006 (1985).

[11] Y. Carmel, V.L. Granatstein and A. Gover, "Demonstration of two-stage backward-wave-oscillator free-electron laser," Phys. Rev. Lett. 51, 566-569 (1983).

[12] L.R. Elias, "High power, efficient, tunable (uv through ir) free electron laser using low energy electron beams", Phys. Rev. Lett. 42, 977-980 (1979).

[13] V.L. Bratman, G.G. Denisov, N.S. Ginzburg, A.V. Smorgonsky, S.D. Korovin, S.D. Polevin, V.V. Rostov and M.I. Yalandin, "Stimulated scattering of waves in microwave generators with high-current relativistic electron beams: simulation of two-stage free-electron lasers," Int. J. Electron., 59, 247-289 (1985).

[14] S. VonLaven, S.B. Segall and J.F. Ward, "A low loss quasioptical cavity for a two stage free electron laser (FEL)", in Free Electron Generators of Coherent Radiation, SPIE vol. 453, page 244-254 (1983).

[15] H.R. Hiddleston, S.B. Segall, and G.C. Catella, "Gain enhanced free electron laser with an electromagnetic pump field", **Physics of Quantum Electronics**, vol.9, 849-865, Addison-Wesley, Reading, Mass. (1982).

[16] J.S. Wurtele, G. Bekefi, B.G. Danly, R.C. Davidson and R.J. Temkin, "Gyrotron electromagnetic wiggler for FEL applications," Bull. Am. Phys. Soc. 30, Paper 655, 1540 (1985).

[17] K.E. Kreischer, B.G. Danly, J.B. Schutkeker and R.J. Temkin, "The design of megawatt gyrotrons," IEEE Trans. Plasma Sci. PS-13, 364-373 (1985).

[18] A. Sh. Fix, V.A. Flyagin, A.L. Goldenberg, V.I. Khiynyak, S.A. Malygin, Sh. E. Tsimring, V.E. Zaperalov, Int. J. Electron. 57, 821-826 (1984).

[19] A. Fruchtman and L. Friedland, "Theory of a nonwiggler collective free electron laser in a uniform magnetic field", IEEE J. Quantum Electron. QE-19, 327-333 (1983).

[20] S.H. Gold, A.W. Fliflet, W.M. Manheimer, W.M. Black, V.L. Granatstein, A.K. Kinkead, D.L. Hardesty and M. Sucy, "High voltage Ka-band gyrotron experiment," IEEE Trans. Plasma Sci. PS-13, 374-382 (1985).

[21] S.N. Voronkov, V.I. Krementsov, P.S. Strelkov and A.G. Shkvarunets, "Stimulated cyclotron radiation at millimeter wavelengths from high power relativistic electron beams," Sov. Phys.-Tech. Phys. 27, 68 (1982).

[22] I.E. Botvinnik, V.L. Bratman, A.B. Volkov, G.G. Denisov, B.D. Kol'chugin, and M.M.

Ofitserov, "The cyclotron autoresonance maser operated at a wavelength 2.4 mm", Sov. Tech. Phys. Lett., 8, 596-597 (1982).

[23] W.B. Colson, "One-body dynamics in a free electron laser", Phys. Lett. 64 A, 190-192 (1977).

[24] E. Jerby and A. Gover, "Investigation of the gain regimes and gain parameters of the free electron laser dispersion equation", IEEE J. Quantum Electron., QE-21, 1041-1058 (1985).

[25] T.I. Smith and J.M.J. Madey, "Realizable free-electron lasers," Appl. Phys. B 27, 195-199 (1982).

[26] N.M. Kroll, P.L. Morton and M.R. Rosenbluth, "Free electron lasers with variable parameter wigglers," IEEE J. Quantum Electron., QE-17, 1436-1468 (1981).

[27] H.P. Freund, R.A. Kehs and V.L. Granatstein, "Electron orbits in combined electromagnetic wiggler and axial guide magnetic fields," IEEE J. Quantum Electron. QE-21, 1080-1082 (1985).

[28] E.T. Scharleman, "Wiggle plane focusing in linear wigglers", J. Appl. Phys. 58, 2154-2161 (1985).

[29] A. Gover and P. Sprangle, "A unified theory of magnetic bremstrahlung, electrostatic bremstrahlung, Compton-Raman scattering, and Cerenkov- Smith-Purcell free electron lasers," IEEE J. Quantum Electron. QE-17, 1196-1215 (1981).

[30] W.B. Colson and P. Elleaume, "Electron dynamics in free electron laser resonator modes," Appl. Phys. B. 29, 101-109 (1982).

[31] C.W. Roberson, "Free electron laser beam quality," IEEE J. Quantum Electron., QE-21, 860-866 (1985), and A.M. Sessler and D. Prosnitz, "Single pass accelerators for FELs", Lawrence Livermore National Laboratory, ELF note No. 114P (1984).

[32] C.E. Hess, H.A. Schwettman and T.I. Smith, "Harmonically resonant cavities for high brightness beams," IEEE Trans. Nucl. Sci., NS-32, 2924-2926 (1985).

[33] R.C. Davidson and H.S. Uhm, "Self consistent Vlasov description of the free electron laser instability", Phys. Fluids 23, 2076-2084 (1980).

[34] P. Sprangle and R.A. Smith, "Theory of free electron lasers", Phys. Rev. A 21, 293-301 (1980).

[35] R.C. Davidson and J.S. Wurtele, "Self consistent kinetic description of the free electron laser instability in a planar magnetic wiggler", IEEE Trans. Plasma Science PS-13, 464-479 (1985).

[36] A.M. Dimos and R.C. Davidson, "Quasilinear stabilization of the free electron laser instability for a relativistic electron beam propagating through a transverse helical wiggler magnetic field", Phys. Fluids 28, 677-694 (1985).

[37] R.E. Collin, **Foundations for Microwave Engineering**, McGraw Hill, 1966.

[38] W.D. Kilpatrick, Rev. Sci. Instrum. 28, 824 (1957).

[39] K. Halbach, "Permanent magnet undulators", J. de Physique, C1, 211-216, (1983).

[40] V.L. Granatstein, W.W. Destler, and I.D. Mayergoyz, "Small period electromagnet wigglers for free electron lasers", Appl. Phys. Lett. 47, 643-645 (1985).

[41] T. Shintake, K. Huke, J. Tanaka, I. Sato, and I. Kumabe, "Development of microwave undulator", Jap. J. Appl. Phys. 22, 844-851 (1983).

[42] B.G. Danly and R.J. Temkin, "Generalized nonlinear harmonic gyrotron theory", Phys. Fluids, 29, 561-567 (1986).

[43] T.A. Hargreaves, K.J. Kim, J.H. McAdoo, S.Y. Park, R.D. Seeley, and M.E. Read, "Experimental study of a single mode quasioptical gyrotron", Int. J. Electron. 57, 977-984 (1984).

[44] V.L. Bratman, G.G. Denisov, N.S. Ginzburg, and M.I. Petelin, "FELs with Bragg reflection resonators: cyclotron autoresonance masers versus ubitrons", J. Quantum Electron. QE-19, 282-296 (1983).

[45] H.R. Jory and A.W. Trivelpiece, "Charged partical motion in large amplitude electromagnetic fields", J. Appl. Phys. 39, 3053-3060 (1968).

[46] D.B. McDermott, D.S. Furuno, and N.C. Luhmann, Jr., "Production of relativistic, rotating electron beams by gyroresonant rf acceleration in a TE_{111} rf cavity", J. Appl. Phys. 58, 4501-4508 (1985).

[47] P. Sprangle, L. Vlahos, and C.M. Tang, "A cyclotron resonance laser accelerator", IEEE Trans. Nucl. Sci., NS-30, 3177-3179 (1983).

Figure Captions

Fig. 1 FEL gain at $\lambda_s = 10\,\mu$m for 30 GHz ($\lambda = 1\,$cm) electromagnetic wiggler ($a_w = 0.05$). Different brightnesses, B_n [kA/cm^{2}rad^2], and number of wiggler periods N are shown.

Fig. 2 FEL gain at $\lambda_s = 10\,\mu$m for 60 GHz ($\lambda = 5\,$mm) electromagnetic wiggler ($a_w = 0.05$). Different brightnesses, B_n [kA/cm^{2}rad^2], and number of wiggler periods N are shown.

Fig. 3 FEL gain at $\lambda_s = 10\,\mu$m for 150 GHz ($\lambda = 2\,$mm) electromagnetic wiggler ($a_w = 0.05$). Different brightnesses, B_n [kA/cm^{2}rad^2], and number of wiggler periods N are shown.

Fig. 4 Distribution function G_0^+ relative to the ponderomotive velocity v_r in the a) monoenergetic limit, and b) the weak resonant growth regime. V_b is the beam velocity.

Fig. 5 Comparison of gain for short wavelength magnetostatic (MS) hybrid wiggler and electromagnetic (EM) wiggler. The following parameters are assumed: $\lambda_s = 10\mu$m, $I = 100$A, $B_n = 240\,$kA/cm^{2}rad^2, and $N = 200$. The voltage (U) required is also shown.

Fig. 6 One possible GEM wiggler FEL configuration

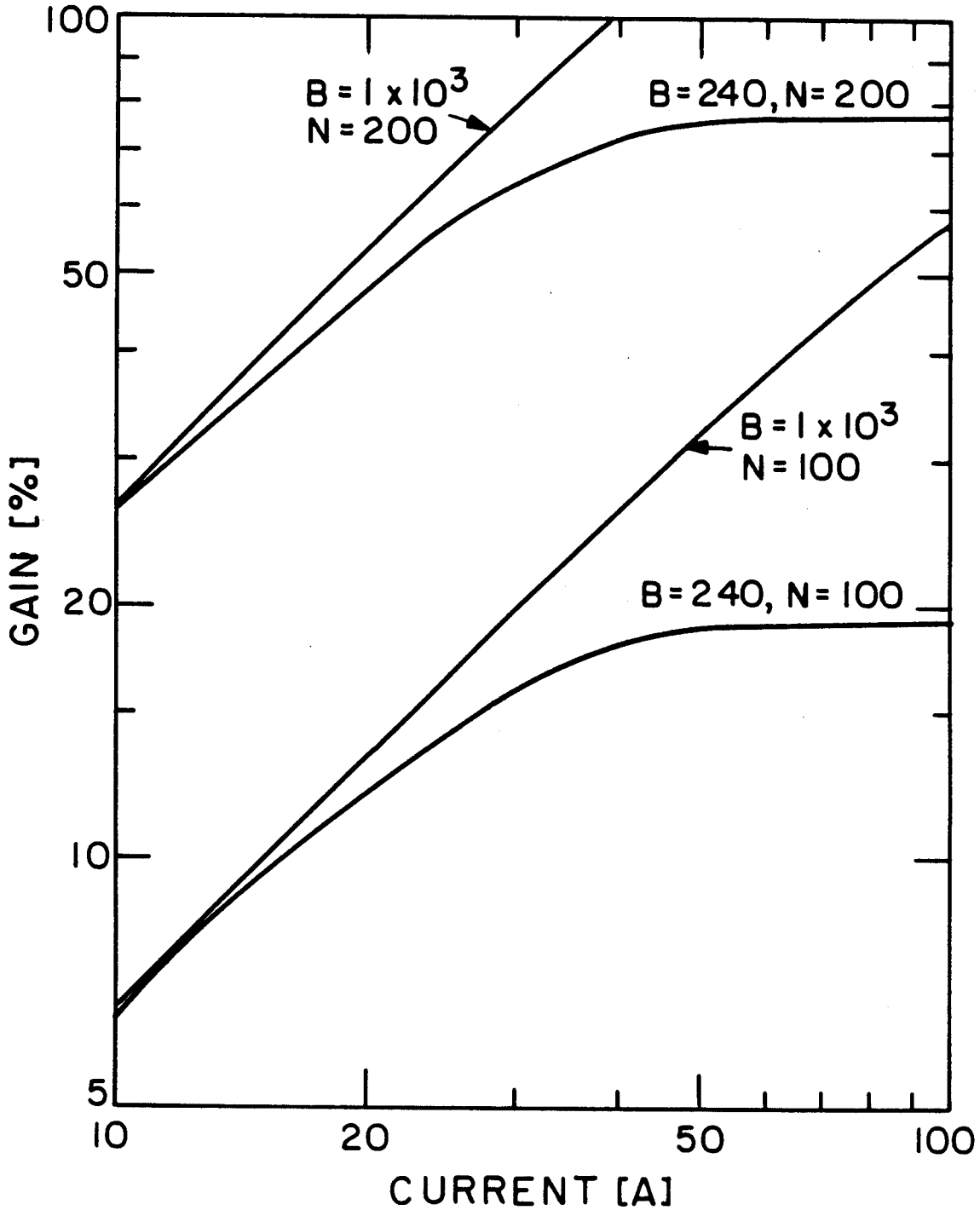
100
50
20
10
5
GAIN [%]
B = 1 x 10^3
N = 200
B = 240, N = 200
B = 1 x 10^3
N = 100
B = 240, N = 100
10
20
50
100
CURRENT [A]

Fig. 1

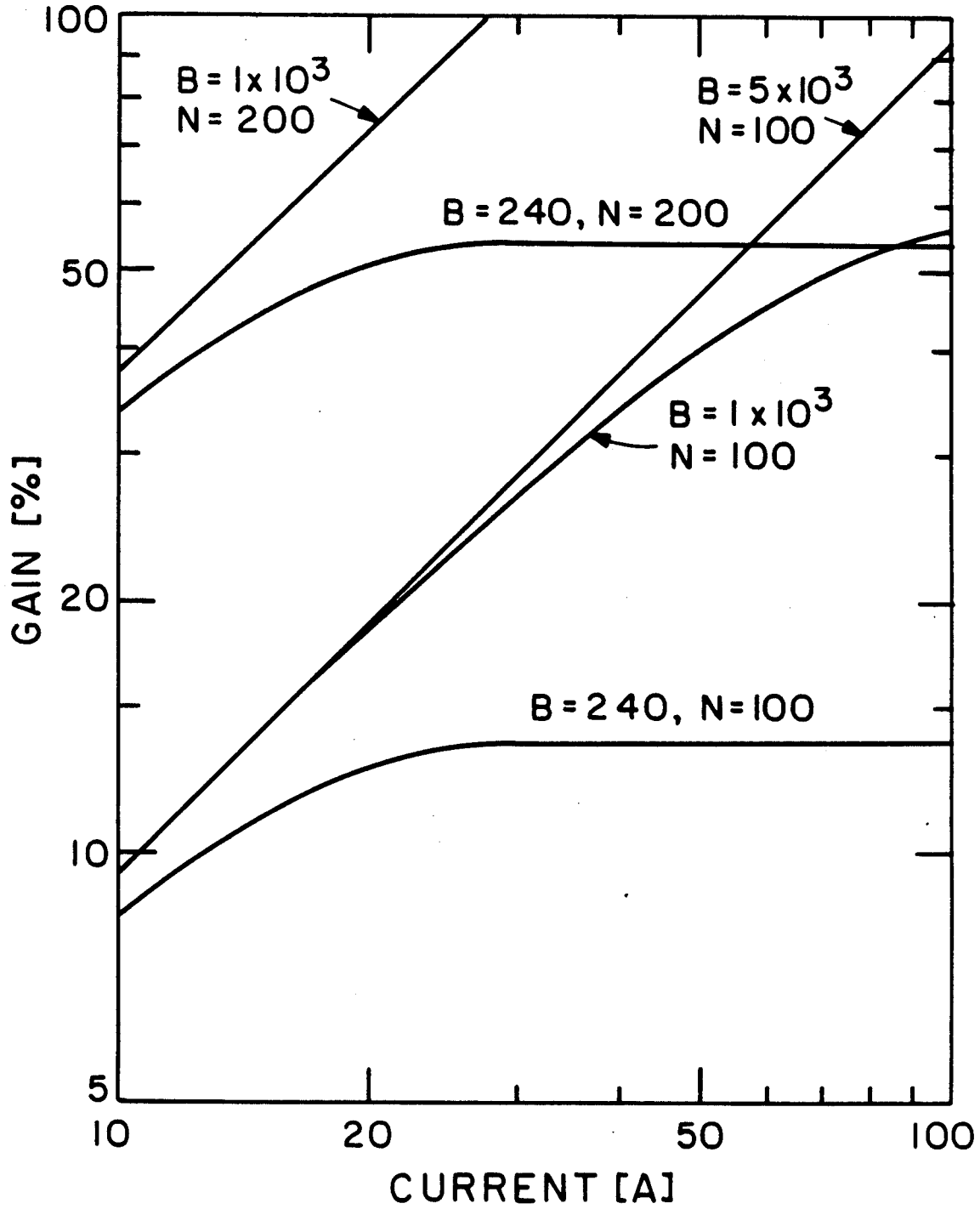
100
50
20
10
5
GAIN [%]
B = 1x10^3
N = 200
B = 5x10^3
N = 100
B = 240, N = 200
B = 1x10^3
N = 100
B = 240, N = 100
10
20
50
100
CURRENT [A]

Fig. 2

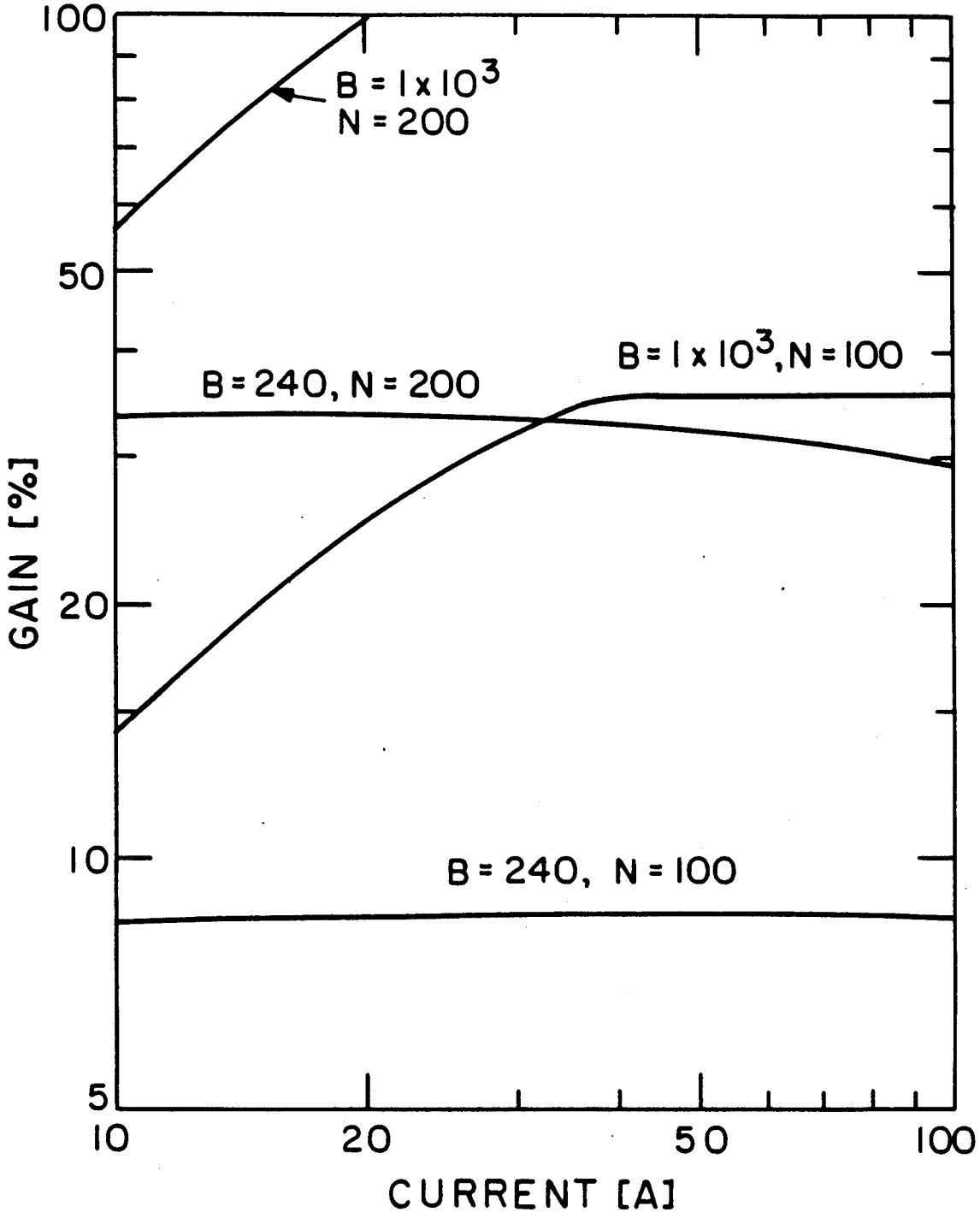
100
50
20
10
5
GAIN [%]
B = 1 x 10^3
N = 200
B = 1 x 10^3, N = 100
B = 240, N = 200
B = 240, N = 100
10
20
50
100
CURRENT [A]

Fig. 3

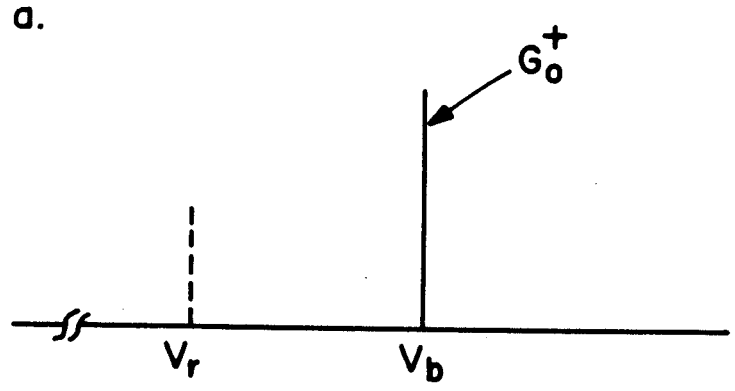

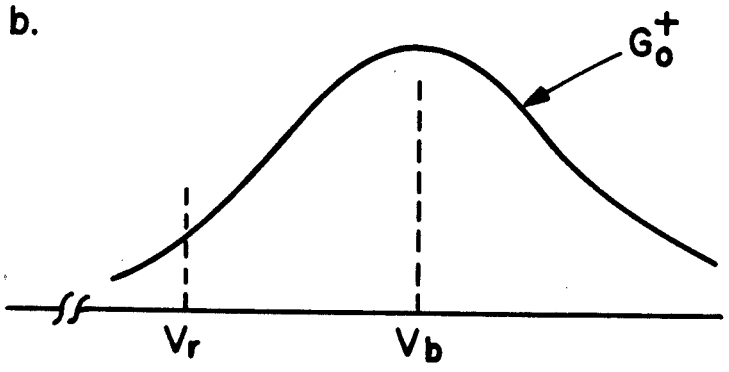

Fig. 4

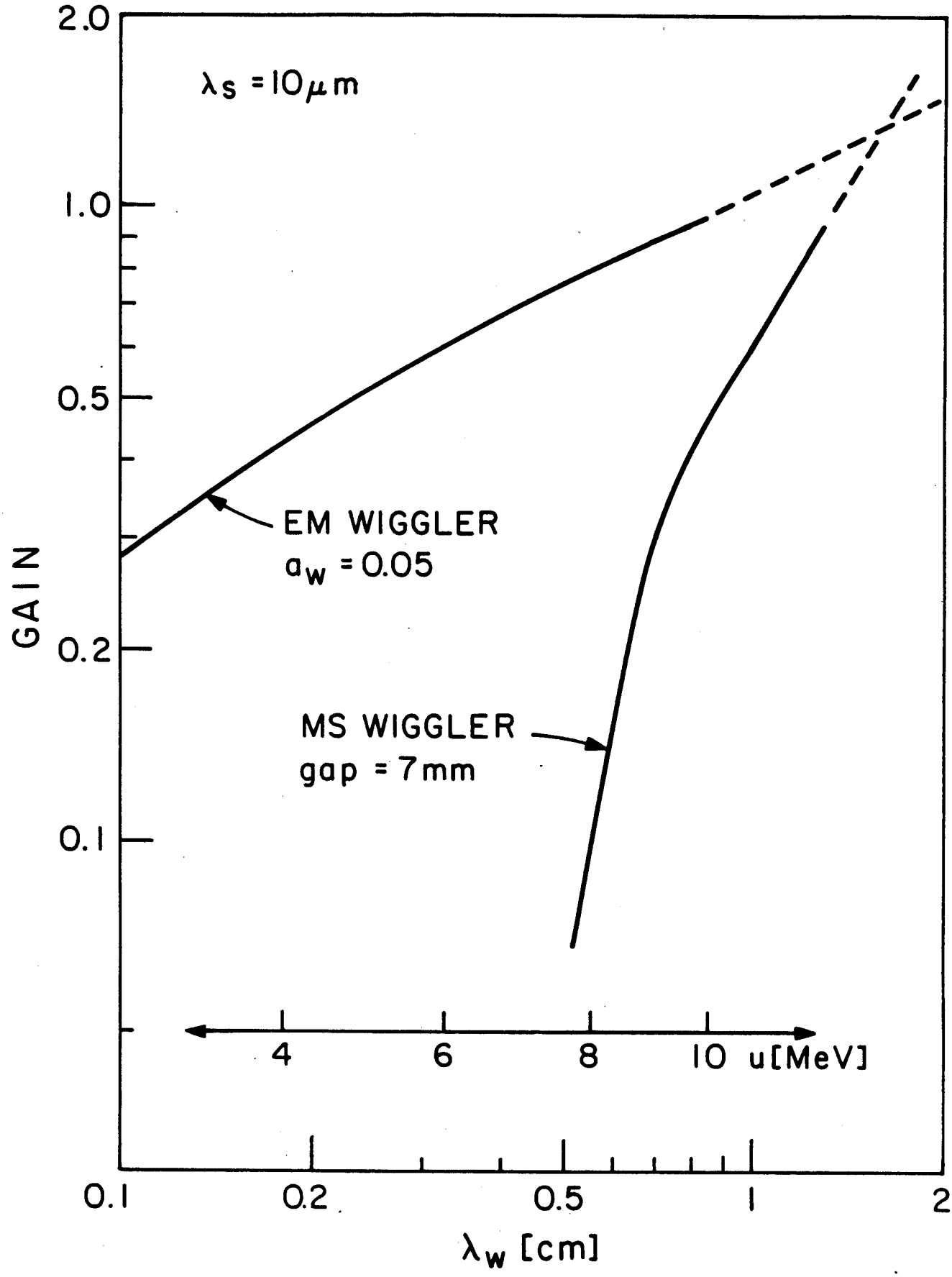
2.0
$\lambda_s = 10\mu m$
1.0
0.5
0.2
0.1
GAIN
EM WIGGLER
$a_w = 0.05$
MS WIGGLER
gap = 7mm
4
6
8
10 u[MeV]
0.1
0.2
0.5
1
2
λ_w [cm]

Fig. 5

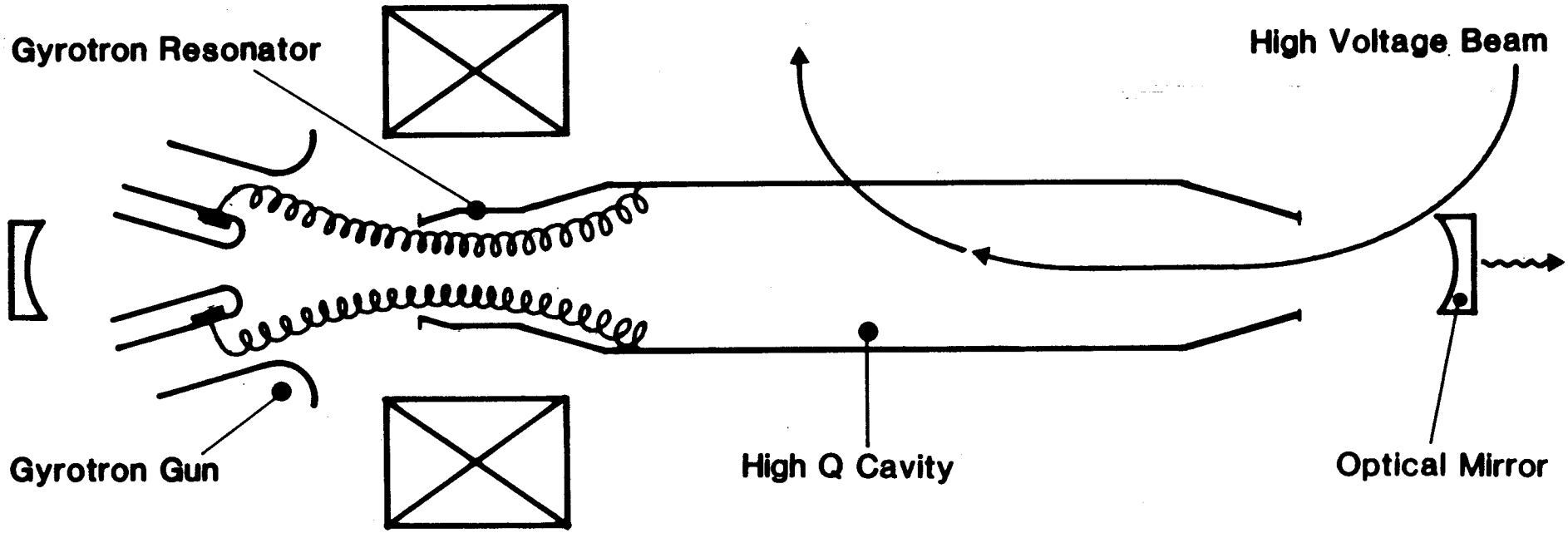
Gyrotron Resonator
High Voltage Beam
Gyrotron Gun
High Q Cavity
Optical Mirror

Fig. 6